
Self-attention Dual Embedding for Graphs with Heterophily

Yurui Lai*, Taiyan Zhang*, Rui Fan

School of Information Science and Technology, ShanghaiTech University, Shanghai, China
 {laiyr, zhangty2022, fanrui}@shanghaitech.edu.cn

Abstract

Graph Neural Networks (GNNs) have been highly successful for the node classification task. GNNs typically assume graphs are homophilic, i.e. neighboring nodes are likely to belong to the same class. However, a number of real-world graphs are heterophilic, and this leads to much lower classification accuracy using standard GNNs. In this work, we design a novel GNN which is effective for both heterophilic and homophilic graphs. Our work is based on three main observations. First, we show that node features and graph topology provide different amounts of informativeness in different graphs, and therefore they should be encoded independently and prioritized in an adaptive manner. Second, we show that allowing negative attention weights when propagating graph topology information improves accuracy. Finally, we show that asymmetric attention weights between nodes are helpful. We design a GNN which makes use of these observations through a novel self-attention mechanism. We evaluate our algorithm on real-world graphs containing thousands to millions of nodes and show that we achieve state-of-the-art results compared to existing GNNs. We also analyze the effectiveness of the main components of our design on different graphs.

1 Introduction

The graph node classification task tries to predict the classes of nodes on the basis of their features and the graph topology. An edge between two nodes indicates the correlation between the classes of the nodes. Many real-world graphs are homophilic[26], meaning there is positive correlation between an edge’s endpoints. However, other graphs are naturally heterophilic, so that edges, while still informative, often indicate negative correlation between the endpoints[43]. For example, in the University of Wisconsin web graph, there are frequently edges between different classes of web pages, for example from a faculty’s homepage to web pages of their students and courses[22].

Graph Neural Network(GNN) achieves great success on node classification[17] [29][33][31][35]. However, standard GNNs implicitly assume graphs are homophilic, because the aggregation step in most GNNs pushes the embeddings of neighboring nodes close to each other, leading to neighbors often receiving the same class. When such GNNs are applied to heterophilic graphs, their accuracy can degrade substantially[22][43][37].

A number of recent works[22][43][4][2][36] [34][21][18][8] focus on improving GNN accuracy on heterophilic graphs . We divide these works into two types, depending on whether they make use of graph topology information in an implicit or explicit manner. To overcome the problems of traditional GNNs, many methods in the first type allow negative attention weights between nodes

*Equal contribution

during aggregation[4][2][36]. Viewing the nodes' classes as a graph signal, these algorithms apply both high and low pass filters on the signal, whereas standard GNNs use only positive attention weights and thus only apply low pass filters. Besides, other techniques such as multi-hop embedding combination [13], node sequence sampling[8], etc. have been used in this type. The first type of algorithm implicitly makes use of the graph topology via message passing along edges. The second type of heterophilic GNNs also use negative attention weights, and additionally make explicit use of topology information by treating each node's adjacency vector, giving its connections to all other nodes, as an additional feature[34][18][21][37]. It embeds nodes using a combination of their standard and adjacency features. This approach is sometimes highly effective and can substantially improve classification accuracy.

In this work, we propose several novel techniques which further increase the accuracy of heterophilic graphs. We first observe that node and topology features provide different degrees of informativeness in different graphs. Thus, when one type of feature is substantially more informative than the other, we should avoid premature mixing of the features to avoid "contamination". Second, we show that using negative attention weights when embedding topology features improves accuracy, in the same way, that such weights are useful when embedding node features. Finally, while existing heterophilic GNNs use only symmetric edge weights, we show that it is beneficial to allow asymmetric attention weights between nodes, i.e. to let one node i influence node j more than j influences i through edges (i, j) and (j, i) with different weights.

Based on these observations, we propose a novel GNN model which we call SADE-GCN (self-attention dual embedding graph convolutional network). SADE-GCN explicitly separates the embeddings of the node and topology features and only combines them in the final step of the model. It allows negative attention weights when computing both node and topology embeddings. Furthermore, it uses a novel self-attention mechanism to enable asymmetric attention weights. We give an efficient implementation of our algorithm on a range of benchmark graphs with thousands to millions of edges. Our algorithm achieves high accuracy on homophilic graphs and is more accurate than all other GNNs on nearly all heterophilic graphs. We conduct a number of ablations to validate different aspects of our design. Results show that the unique aspects of our model often substantially improve accuracy.

In summary, our contributions are as follows.

- We observe that the importance of topology and feature varies among graphs, and show that using negative attention weights when embedding topology features improves accuracy for heterophilic graphs. Additionally, we highlight the benefits of using asymmetric attention weights between neighbors.
- To leverage our observations, we propose a new model called SADE-GCN. This model is based on Dual Embedding architecture that keeps the independence of feature and topology during message passing. Furthermore, SADE-GCN incorporates a novel self-attention mechanism that extracts the heterophily and asymmetry of the graph.
- Finally, we assess the effectiveness of SADE-GCN on a total of 13 graphs, including 10 heterophilic and 3 homophilic ones. We demonstrate that our proposed model outperforms other existing state-of-the-art methods in terms of prediction accuracy. Furthermore, our experiments also show that our proposed method can be readily extended to handle large-scale graphs. Additionally, we investigate the contributions of individual modules by conducting ablation experiments.

2 Preliminaries

We introduce notations and background knowledge in this section. A graph $\mathcal{G} = (\mathcal{V}, \mathcal{E})$, \mathcal{V} is node set and \mathcal{E} is edge set. There are N nodes and E edges in a graph. We denote graph adjacency matrix as $\mathbf{A} \in \mathbb{R}^{N \times N}$. The degree matrix of graph is $\mathbf{D} \in \mathbb{R}^{N \times N}$. The node feature is $\mathbf{X} \in \mathbb{R}^{N \times F}$ and node label is $\mathbf{Y} \in \mathbb{R}^{N \times C}$, where C is the number of classes.

2.1 Graph Neural Network

Traditional GNNs rely on the message passing mechanism, which entails two phases: aggregation and transformation. During the aggregation phase, the embeddings are propagated along an adjacency

matrix. Then, embeddings after propagation are transformed by non-linear or linear layers. The mechanism can be recursively defined as follows.

$$\mathbf{H}^{(0)} = \mathbf{X}, \quad \mathbf{H}^{(l)} = \sigma(\tilde{\mathbf{A}}\mathbf{H}^{(l-1)}\mathbf{W}^{(l)}) \quad (1)$$

where the hidden feature embedding of l layer of GNN is $\mathbf{H}^l \in \mathbb{R}^{N \times F^{(l)}}$ and σ is non-linear function. $\tilde{\mathbf{A}}$ represents $\mathbf{D}^{-1}\mathbf{A}$, $\mathbf{D}^{-1/2}\mathbf{A}\mathbf{D}^{-1/2}$, etc. Since the normalized adjacency is a low-pass filter[2], the embeddings of neighboring nodes tend to become more similar. When the heterophily is high, nodes of different classes often have similar embeddings, which subsequently leads to a significant reduction in GNN performance.

2.2 Self-attention in Transformer

The transformer was first proposed in natural language processing [28] and has since gained popularity with great success in other fields, such as computer vision [5][11] and bioinformatics [27][14]. Recently, transformers have also achieved success on graph applications [39][40][38][25]. The fundamental element of graph transformers is self-attention. Let hidden embedding of l layer of transformer be $\mathbf{H}^{(l)} \in \mathbb{R}^{N \times H^{(l)}}$. For layer l , let query weight, key weight and value weight be $\mathbf{W}_Q^{(l)}, \mathbf{W}_K^{(l)}, \mathbf{W}_V^{(l)} \in \mathbb{R}^{H^{(l-1)} \times H^{(l)}}$ respectively, then self-attention can be expressed as

$$\mathbf{Q}^{(l)} = (\mathbf{H}^{(l-1)}\mathbf{W}_Q^{(l)}), \quad \mathbf{K}^{(l)} = (\mathbf{H}^{(l-1)}\mathbf{W}_K^{(l)}), \quad \mathbf{V}^{(l)} = (\mathbf{H}^{(l-1)}\mathbf{W}_V^{(l)}), \quad (2)$$

$$\mathbf{H}^{(l)} = \text{Softmax}\left(\frac{(\mathbf{Q}^{(l)})(\mathbf{K}^{(l)})^T}{\sqrt{H^{(l)}}}\right)(\mathbf{V}^{(l)}) + \text{Res}(\mathbf{H}^{(0)}) \quad (3)$$

Here, $\text{Res}()$ denotes the residual connection function[12][28], and $\mathbf{H}^{(0)}$ denotes the graph embedding. The self-attention mechanism calculates the pairwise inner product between the input elements from the query \mathbf{Q}^{l-1} and the key \mathbf{K}^{l-1} matrices. The output is obtained by taking the weighted average of \mathbf{V}^{l-1} .

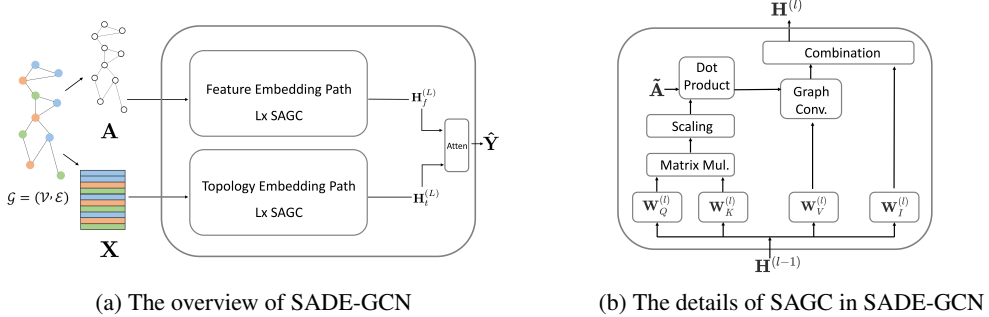


Figure 1: Our method

3 Self-attention Dual Embedding

This section presents an overview of our proposed method, SADE-GCN (self-attention dual embedding graph convolutional network), which is based on our three observations of heterophilic graphs and detailed analysis.

3.1 Observations of Heterophilic Graphs

3.1.1 Different Importance of Feature and Topology

As recent research [37] demonstrates, heterophilic graphs require a compromise between graph topology and node features. It is thus crucial to explicitly encode both feature and topology information in order to achieve effective performance. To that end, some existing GNN approaches for heterophilic graphs, such as [34], [18], and [21], emphasize the importance of explicitly embedding topology information and then combining it with feature embedding during message passing.

To evaluate the relative importance of feature and topology information in graphs, we conducted experiments for graph node classification using both MLP and LINK[42]. MLP solely relies on feature information, while LINK is a model with a linear layer that takes the adjacency matrix as input, with each row of the matrix representing the topology of the corresponding node. MLP outperforms LINK on some heterophilic graphs, such as Wisconsin, achieving an accuracy of 85.29% compared to 51.96% with LINK, indicating that feature information is more important in those cases. However, on other graphs, including Chameleon, MLP underperforms relative to LINK, achieving an accuracy of only 46.21% compared to 70.57% using LINK, demonstrating the greater importance of topology information in those cases. The full results of these experiments are presented in Tables 2 and 3. These results suggest that the relative importance of feature and topology information varies among graphs. We hypothesize that the different levels of noise in feature and topology may correspond to their different importance. Thus, we propose keeping the independence of feature and topology embeddings during message passing as a way to enhance the model’s robustness to noise and boost overall performance. This approach is consistent with some prior work that acknowledges the presence of inherent noise in both feature and topology information [41][30].

3.1.2 Graph Topology for Heterophily

From the perspective of graph signal processing, the raw adjacency matrix is a low-frequency filter that only captures the homophily of a graph [2][21]. To account for heterophily, GNNs leverage high-frequency filters by introducing negative edge weights to the adjacency matrix. Specifically, when adjacent nodes with different class labels are connected by negative weights, the distance between the feature embeddings of these nodes increases.

Previous studies have emphasized the role of feature embeddings in capturing heterophily [2][21]. However, for effective extraction of heterophily, it is crucial to make use of both topology and feature information. In order to achieve this, we propose employing attention matrices for feature and topology embeddings respectively.

3.1.3 Asymmetry of Heterophilic Graph

In reality, neighbors in a heterophilic graph often possess varying influences over each other. For example, in fraudulent networks[6], fraudsters often establish connections with regular users. Regular users tend to assume that fraudsters are also regular users, while fraudsters are unlikely to make the same mistake. Therefore, it’s necessary to capture the asymmetry in influence.

Traditional GNNs like GCN usually convert the input to a symmetric undirected graph. In [34][21][10], an attention matrix representing the interaction between neighbors is used to adjust the adjacency matrix for message passing. The calculation of the attention matrix typically involves the computation of similarity measures such as cosine distance and inner product, which by design, are symmetric. An attention matrix with greater expressiveness and asymmetry is needed to more accurately adjust the weights of edges in the network.

3.2 Dual Embedding Paths

SADE-GCN consists of two parallel paths to embed features and topology independently. One is \mathbf{P}_f which explicitly embeds features. It takes node features as input. Similarly, \mathbf{P}_t captures topology information explicitly. There exist several techniques for embedding graph topology [21][32][7]. In this study, we adopt the adjacency matrix as the input for \mathbf{P}_t . Each row of the adjacency matrix represents the topology of a node. Both paths through the network consist of SAGC (self-attention graph convolution) modules, which are introduced in the next section.

3.3 Self-attention Graph Convolution

3.3.1 Self-attention for Graphs with Heterophily

Firstly, we use self-attention to obtain the attention matrix. Self-attention has strong expressive power [19][24][23][15], making it well-suited for capturing complex patterns within a graph network. To the best of our knowledge, this is the first application of self-attention in heterophilic graphs.

For \mathbf{P}_f , the query $\mathbf{W}_{Q_f}^{(l)}$ and key weight $\mathbf{W}_{K_f}^{(l)} \in \mathbb{R}^{H^{(l-1)} \times H_{K_f}^{(l)}}$. For \mathbf{P}_t , the query $\mathbf{W}_{Q_t}^{(l)}$ and key weight $\mathbf{W}_{K_t}^{(l)} \in \mathbb{R}^{H^{(l-1)} \times H_{Q_f}^{(l)}}$. \mathbf{P}_f and \mathbf{P}_t have the same embedding mechanism. We use a unified framework to describe the process.

We can get the query and key for feature and topology in equation 4. The attention matrix with positive value $\mathbf{R}_f^{(l)}$ and $\mathbf{R}_t^{(l)}$ are respectively calculated by matrix multiplication of query and key in equation 5.

$$\mathbf{Q}^{(l)} = \text{Softmax}(\mathbf{H}^{(l-1)} \mathbf{W}_Q^{(l)}), \quad \mathbf{K}^{(l)} = \text{Softmax}(\mathbf{H}^{(l-1)} \mathbf{W}_K^{(l)}) \quad (4)$$

$$\mathbf{R}^{(l)} = \mathbf{Q}^{(l)} (\mathbf{K}^{(l)})^T \quad (5)$$

Here we introduce modifications to the standard self-attention mechanism. Specifically, we perform a Softmax operation on the query and key vectors prior to multiplication. This modification is necessary because the graphs are often large and sparse, we only need to focus on neighboring nodes. If we perform a Softmax operation on each row of the attention matrix, as in the standard self-attention mechanism, the attention weights for neighboring nodes will be excessively small due to interference from a large number of non-neighbor nodes.

The values of $\mathbf{R}^{(l)}$ generated through our SADE-GCN model exist within the range of $[0, 1]$. However, in order to accurately capture the heterophily of the graph network, it is necessary to include negative attention weights. To achieve this, we employ a scaling function, as defined in equation 6, to map the values of $\mathbf{R}^{(l)}$ from the range of $[0, 1]$ to $[-1, 1]$. Subsequently, we utilize the attention matrices to reweight the edge weights through element-wise multiplication, also known as the Hadamard Product equation 7. Through this operation, our model selectively accounts only for neighboring nodes, thereby setting all non-neighbor attention weights to zero. In this way, we obtain $\tilde{\mathbf{A}}_f^{(l)}$ and $\tilde{\mathbf{A}}_t^{(l)}$ values for the feature and topology paths, respectively.

$$\hat{\mathbf{R}}^{(l)} = 2\mathbf{R}^{(l)} - 1 \quad (6)$$

$$\tilde{\mathbf{A}}^{(l)} = \hat{\mathbf{R}}^{(l)} \odot \mathbf{A} \quad (7)$$

We provide an efficient implementation to obtain the reweighted adjacency matrix $\tilde{\mathbf{A}}$ for large graphs containing hundreds of thousands of nodes. Details of this implementation can be found in the Appendix. In summary, our approach directly calculates the attention weights of neighbors instead of removing the non-neighbors after applying self-attention.

3.3.2 Heterophilic Graph Convolution

We give heterophilic graph convolution after getting the reweighted adjacency matrix. For feature, the value weight is $\mathbf{W}_{V_f}^{(l)}$ and residual weight is $\mathbf{W}_{I_f}^{(l)} \in \mathbb{R}^{H^{(l-1)} \times H^{(l)}}$. For topology, the value weight is $\mathbf{W}_{V_t}^{(l)}$ and residual weight is $\mathbf{W}_{I_t}^{(l)} \in \mathbb{R}^{H^{(l-1)} \times H^{(l)}}$.

$$\mathbf{H}^{(l)} = \alpha_V \mathbf{c}_V \text{ReLU}(\tilde{\mathbf{A}}^{(l)} \mathbf{H}^{(l-1)} \mathbf{W}_V^{(l)}) + \alpha_I \mathbf{c}_I \mathbf{H}^{(l-1)} \mathbf{W}_I^{(l)} \quad (8)$$

$$\mathbf{c}_V, \mathbf{c}_I = \text{Softmax}(\sigma(\mathbf{H}^{(l)} \mathbf{G}_V), \sigma(\mathbf{H}^{(l)} \mathbf{G}_I)) \quad (9)$$

where \mathbf{G}_V and \mathbf{G}_I are learnable weights, α_V and α_I are hyperparameters used for manually weighing the message passing and residual result. σ here is a sigmoid layer.

3.3.3 Feature and Topology Embedding Combination

The final output $\hat{\mathbf{Y}} \in \mathbb{R}^{N \times C}$ comes from an adaptive combination of two paths output $\mathbf{H}_f^{(L)}$ and $\mathbf{H}_t^{(L)}$, where L represents length of the embedding path.

$$\hat{\mathbf{Y}} = \alpha_f \mathbf{c}_f \mathbf{H}_f^{(L)} + \alpha_t \mathbf{c}_t \mathbf{H}_t^{(L)} \quad (10)$$

where \mathbf{c}_f and \mathbf{c}_t are attention vectors, which are calculated in the same way as the above method. α_f and α_t are hyperparameters used for manually weighing features and topology embedding.

4 Experiment

In this section, we first present our experimental settings. Next, we evaluate our method for node classification on several real-world graph datasets and compare it with state-of-the-art (SOTA) methods. Finally, we analyze the components of our method, as well as confirm the observations and analysis presented in the previous section.

4.1 Settings

4.1.1 Datasets

We adopt a total of 13 real-world graph datasets in our experiments. The Cora, Citeseer, and PubMed datasets[26] are citation networks with high homophily. In [22], a series of heterophilic graphs are proposed, including the Texas, Wisconsin, Cornell, Wikipedia networks Squirrel and Chameleon, and Actor co-occurrence network. These nine datasets are commonly used in research on heterophilic graphs. However, their scales are relatively small, ranging from a few hundred to a few thousand nodes and from a few hundred to tens of thousands of edges. Recently, in [20], large-scale heterophilic graphs with up to millions of nodes and tens of millions of edges were introduced, which pose additional challenges. Thus, we include Penn94, arXiv-year, genius, and twitch-gamers from [20] in our experiments. These graphs vary in feature dimension, homophily level, and number of nodes and edges, enabling us to fully test the ability of our model. We provide the characteristics of these graphs in Table 1, with additional descriptions available in the Appendix.

Table 1: The overview of 13 graph datasets’ characteristics. The edge homophily is measured by the ratio of the edges that connect nodes with the same label.

	Texas	Wisconsin	Cornell	Film	Squirrel	Chameleon	Cora	Citeseer	Pubmed	Penn94	arXiv-year	genius	twitch-gamers
Nodes	183	251	183	7,600	5,201	2,277	2,708	3,327	19,717	41,554	169,343	421,967	168,114
Edges	295	466	280	26,752	198,493	31,421	5,278	4,676	44,327	1,362,229	1,166,243	984,979	6,797,557
Features	1,703	1,703	1,703	931	2,089	2,325	1,433	3,703	500	5	128	12	7
Classes	5	5	5	5	5	5	6	7	3	2	5	2	2
Edge Hom.	0.11	0.21	0.30	0.22	0.22	0.23	0.81	0.74	0.80	0.47	0.22	0.61	0.54

Table 2: The overall accuracy results of the compared methods on the 9 small datasets. We highlight the best score on each dataset in bold and the second is underlined. Note that the error bar (\pm) indicates the standard deviation score of the results over.

	Cora	Citeseer	Pubmed	Squirrel	Chameleon	Texas	Wisconsin	Cornell	Film	Avg-Rank
MLP	75.69 ± 2.00	74.02 ± 1.90	87.16 ± 0.37	28.77 ± 1.56	46.21 ± 2.99	80.81 ± 4.75	85.29 ± 3.31	81.89 ± 6.40	36.53 ± 0.70	13.67
LINK	77.46 ± 1.94	66.16 ± 2.92	78.74 ± 0.47	62.31 ± 1.78	70.57 ± 2.00	58.10 ± 6.75	51.96 ± 5.63	50.54 ± 5.92	24.11 ± 0.70	15.22
GCN	86.89 ± 1.27	76.50 ± 1.36	88.42 ± 0.50	53.43 ± 2.01	64.82 ± 2.24	55.14 ± 5.16	51.76 ± 3.06	60.54 ± 5.30	27.32 ± 1.10	14.56
GAT	87.30 ± 1.10	76.55 ± 1.23	86.33 ± 0.48	40.72 ± 1.55	60.26 ± 2.50	52.16 ± 6.63	49.41 ± 4.09	61.89 ± 5.05	27.44 ± 0.89	15.89
GraphSAGE	86.90 ± 1.04	76.04 ± 1.30	88.45 ± 0.50	41.61 ± 0.74	58.73 ± 1.68	82.43 ± 6.14	81.18 ± 5.56	75.95 ± 5.01	34.23 ± 0.99	13.33
MixHop	87.61 ± 0.85	76.26 ± 1.33	85.31 ± 0.61	43.80 ± 1.48	60.50 ± 2.53	77.84 ± 7.73	75.88 ± 4.90	73.51 ± 6.34	32.22 ± 2.34	14.11
GCNII	88.37 ± 1.25	77.33 ± 1.48	90.15 ± 0.43	38.47 ± 1.58	63.86 ± 3.04	77.57 ± 3.83	80.39 ± 3.40	77.86 ± 3.79	37.44 ± 1.30	8.11
H ₂ GCN	87.87 ± 1.20	77.11 ± 1.57	89.49 ± 0.38	36.48 ± 1.86	60.11 ± 2.15	84.86 ± 7.23	87.65 ± 4.98	82.70 ± 5.28	35.70 ± 1.00	9.67
FAGCN	88.05 ± 1.57	77.07 ± 2.05	88.09 ± 1.38	30.83 ± 0.69	46.07 ± 2.11	76.49 ± 2.87	79.61 ± 1.58	76.76 ± 5.87	34.82 ± 1.35	13.22
GPR-GNN	87.95 ± 1.18	77.13 ± 1.67	87.54 ± 0.38	46.31 ± 2.46	62.59 ± 2.04	81.35 ± 5.32	82.55 ± 6.23	78.11 ± 6.55	35.16 ± 0.90	10.67
WRGAT	88.20 ± 2.26	76.81 ± 1.89	88.52 ± 0.92	48.85 ± 0.78	65.24 ± 0.87	83.62 ± 5.50	86.98 ± 3.78	81.62 ± 3.90	36.53 ± 0.77	8.44
ACM-GCN	87.91 ± 0.95	77.32 ± 1.70	90.00 ± 0.52	54.40 ± 1.88	66.93 ± 1.85	87.84 ± 4.40	88.43 ± 3.22	85.14 ± 6.07	36.28 ± 1.09	5.78
Geom-GCN	85.35 ± 1.57	78.02 ± 1.15	89.95 ± 0.47	38.15 ± 0.92	60.00 ± 2.81	66.76 ± 2.72	64.51 ± 3.66	60.54 ± 3.67	31.59 ± 1.15	13.33
LINKX	87.86 ± 0.77	73.19 ± 0.99	87.86 ± 0.77	61.81 ± 1.80	68.42 ± 1.38	74.60 ± 8.37	75.49 ± 5.72	77.84 ± 5.81	36.10 ± 1.55	11.89
GGCN	87.95 ± 1.05	77.14 ± 1.45	89.15 ± 0.37	55.17 ± 1.58	71.14 ± 1.84	84.86 ± 4.55	86.86 ± 3.29	85.68 ± 6.63	37.54 ± 1.56	6.11
GloGNN	88.31 ± 1.13	77.41 ± 1.63	89.62 ± 0.35	57.54 ± 1.39	69.78 ± 2.42	84.32 ± 4.15	87.06 ± 3.53	83.51 ± 4.26	37.35 ± 1.30	5.78
GloGNN++	88.33 ± 1.09	77.22 ± 1.78	89.24 ± 0.39	57.88 ± 1.76	71.21 ± 1.84	84.05 ± 4.90	88.04 ± 3.22	85.95 ± 5.10	37.70 ± 1.40	4.00
ACM-GCN+	88.05 ± 0.99	77.67 ± 1.19	89.82 ± 0.41	66.98 ± 1.71	74.47 ± 1.84	88.38 ± 3.64	88.43 ± 2.39	85.68 ± 4.84	36.26 ± 1.34	3.78
SADE-GCN	87.93 ± 0.91	77.45 ± 1.82	90.07 ± 0.46	68.20 ± 1.57	75.57 ± 1.57	86.49 ± 5.12	88.63 ± 4.54	86.21 ± 5.59	37.91 ± 0.97	2.44

4.1.2 Baselines

The baseline models can be divided into four categories. The first category consists of MLP and LINK. MLP uses feature information exclusively, while LINK [42] only incorporates topology information. The second category includes traditional GNNs, such as GCN [17], GAT [29], GraphSAGE [9], MixHop [1], and GCNII [3]. The third category encompasses GNNs designed for heterophily but does not explicitly encode topology information, such as H₂GCN [43], FAGCN [2], GPR-GNN [4], WRGAT [18], and ACM-GCN [21]. The fourth category includes heterophilic graph neural networks that explicitly encode topology information, such as LINKX [20], GGCN [37], GloGNN and GloGNN++ [18], and ACM-GCN+ [21]. We obtain the baseline accuracies from [18], except

Table 3: The overall accuracy results of the compared methods on 4 large datasets.

	Penn94	arXiv-year	genius	twitch-gamers	Avg-Rank
MLP	73.61 ± 0.40	36.70 ± 0.21	86.68 ± 0.09	60.92 ± 0.07	12.75
LINK	80.79 ± 0.49	53.97 ± 0.18	73.56 ± 0.14	64.85 ± 0.21	9.75
GCN	82.47 ± 0.27	46.02 ± 0.26	87.42 ± 0.37	62.18 ± 0.26	9.75
GAT	81.53 ± 0.55	46.05 ± 0.51	55.80 ± 0.87	59.89 ± 4.12	11.75
MixHop	83.47 ± 0.71	51.81 ± 0.17	90.58 ± 0.16	65.64 ± 0.27	5.75
GCNII	82.92 ± 0.59	47.21 ± 0.28	90.24 ± 0.09	63.39 ± 0.61	7.75
H_2 GCN	81.31 ± 0.60	49.09 ± 0.10	OOM	OOM	12.00
GPR-GNN	81.38 ± 0.16	45.07 ± 0.21	90.05 ± 0.31	61.89 ± 0.29	10.5
WRGAT	74.32 ± 0.53	OOM	OOM	OOM	14.25
ACM-GCN	82.52 ± 0.96	47.37 ± 0.59	80.33 ± 3.91	62.01 ± 0.73	9.50
LINKX	84.71 ± 0.52	56.00 ± 1.34	90.77 ± 0.27	66.06 ± 0.19	4.00
GGCN	OOM	OOM	OOM	OOM	14.75
ACM-GCN+	84.67 ± 0.68	51.94 ± 0.28	89.72 ± 0.62	65.20 ± 0.16	6.25
GloGNN	85.57 ± 0.35	54.68 ± 0.34	90.66 ± 0.11	66.19 ± 0.29	3.50
GloGNN++	85.74 ± 0.42	54.79 ± 0.25	90.91 ± 0.13	66.34 ± 0.29	2.25
SADE-GCN	86.03 ± 2.12	60.74 ± 3.32	91.24 ± 0.70	66.95 ± 1.89	1.00

for ACM-GCN+, which was not evaluated in [18]. We used the scores for ACM-GCN+ on the nine small graphs from [21] and reproduced them for the four large graphs in our experiments.

4.1.3 Implementation Details

For the nine small-scale datasets, we employ 10 public splits from [22], reserving 48% of nodes for training, 32% for validation, and 20% for testing in each split. As for the four large-scale datasets, we use the five splits provided by [20], which reserve 50% of nodes for training, 25% for validation, and 25% for testing. The average test accuracy and standard deviation for each dataset are reported in our experiments. For the small graphs, we utilize SADE-GCN with two layers and 64 hidden dimensions, while for the large graphs, we implement one layer with 256 hidden dimensions. The cross-entropy loss is used for training SADE-GCN on the node classification task, and we optimize it using Adam [16]. The complete hyperparameter settings can be found in the Appendix.

4.2 Results

4.2.1 Node Classification

We present the results of our method and other baselines on the node classification task in Table 2 and Table 3. The results can be summarized as follows.

Traditional GNNs, such as GCN, GAT, and GraphSAGE, perform poorly on all heterophilic graphs and achieve better results on homophilic graphs. GCNII performs relatively well on heterophilic graphs and achieves state-of-the-art (SOTA) results on two homophilous graphs (Cora and PubMed) due to its initial residual and identity mapping.

Early heterophilic GNNs, such as Geom-GCN, have made less progress than traditional GNNs. H_2 GCN, WRGAT, and GGNN perform well on small-scale heterophilic graphs, but they exceed GPU memory limitations when dealing with large-scale graphs. The ACM family and the GloGNN family have achieved great success on both heterophilic and homophilous graphs, showing that negative attention weights can be helpful. The average ranking of heterophilic graph neural networks with explicitly encoded topology information is significantly better than those without. Although LINKX explicitly encodes topology and feature information, its pure MLP architecture lacks the ability to fully extract heterophily.

Our SADE-GCN achieves SOTA on both small and large graphs with varying levels of heterophily. We find that SADE-GCN performs better than MLP, LINK, and LINKX on every dataset, indicating that our method fully explores and combines feature and topology instead of compromising either. Our model has a significant advantage over other methods for graphs dominated by topology, such as Squirrel, Chameleon, and arXiv-year. This is because our dual embedding architecture and innovative self-attention mechanism unleash the potential of topological information, helping to extract the heterophily of graphs. Our method outperforms FAGCN, which uses an additive attention mechanism, demonstrating the superiority of self-attention for graph data. However, all methods perform poorly on the Film dataset due to the poor quality of its feature and topology.

4.2.2 Ablation Study

the Importance of Feature and topology Information In this section, we analyze the impact of explicitly encoding the feature and topology information. We conducted ablation studies by removing either the feature embedding path \mathbf{P}_f (W/o feature embedding) or the topology embedding path \mathbf{P}_t (W/o topology embedding) in our SADE-GCN model. Our results indicate that SADE-GCN W/o feature performs better than SADE-GCN W/o topology on Cora, Squirrel, Penn94 and Chameleon, while the opposite result is observed for other datasets. This overall corresponds to the importance of feature and topology embedding shown by MLP and LINK.

Table 4: Ablation study for SADE-GCN.

	Cora	Citeseer	Squirrel	Chameleon	Texas	Wisconsin	Cornell	Penn94	genius
W/o feature embedding	83.76 \pm 1.22	68.78 \pm 2.95	67.71 \pm 1.49	74.80 \pm 0.98	64.59 \pm 5.59	57.45 \pm 4.96	54.59 \pm 3.37	85.93 \pm 1.35	90.66 \pm 0.52
W/o topology embedding	87.64 \pm 0.74	77.57 \pm 1.57	48.76 \pm 1.83	63.83 \pm 2.04	84.86 \pm 5.29	86.66 \pm 3.01	85.67 \pm 4.84	85.30 \pm 1.43	90.39 \pm 0.83
W/o feature scaling	86.27 \pm 1.53	76.77 \pm 1.53	68.07 \pm 1.55	74.82 \pm 1.00	83.24 \pm 5.37	84.90 \pm 4.02	84.86 \pm 6.64	84.31 \pm 1.31	90.68 \pm 0.59
W/o topology scaling	87.38 \pm 0.66	77.52 \pm 1.88	68.00 \pm 1.81	75.04 \pm 1.10	81.62 \pm 7.43	85.68 \pm 5.95	85.13 \pm 5.57	84.57 \pm 1.91	90.89 \pm 0.62
SADE-GCN-sym	87.54 \pm 1.24	77.26 \pm 1.27	67.72 \pm 1.92	74.64 \pm 1.78	82.43 \pm 5.30	85.88 \pm 3.48	83.51 \pm 6.66	85.66 \pm 1.50	91.09 \pm 0.74
SADE-GCN	87.93 \pm 0.91	77.45 \pm 1.82	68.20 \pm 1.57	75.57 \pm 1.57	86.49 \pm 5.12	88.63 \pm 4.54	86.21 \pm 5.59	86.03 \pm 2.12	91.24 \pm 0.70
Graph Asymmetry	0.27	0.22	0.57	0.40	0.45	0.39	0.39	0.35	0.37

the Importance of Scaling for Heterophily In this section, we explore the impact of feature and topology heterophily on the performance of SADE-GCN. The scaling function in equation 6 makes SADE-GCN have attention matrices with negative values to extract heterophily from feature and topology. We remove it from the embedding path \mathbf{P}_f , \mathbf{P}_t for ablation. The result is in Table 4, W/o feature (topology) scaling corresponds to removing the scaling function from \mathbf{P}_f (\mathbf{P}_t). we find that the absence of either will result in performance degradation. The more important the embedding is, the larger degradation when the scaling function is absent.

the Importance of Asymmetric Attention Matrix In this section, we analyze the asymmetric attention matrix of our model and propose a new variant of SADE, named SADE-GCN-sym, as a comparison. SADE-GCN-sym obtains a symmetric attention matrix through the inner product of the embeddings and their transposition. We introduce the concept of graph asymmetry, which quantifies the relative difference between the attention values of neighboring nodes. Specifically, the relative difference is defined as $\frac{|\hat{\mathbf{R}}_{ij} - \hat{\mathbf{R}}_{ji}|}{|\hat{\mathbf{R}}_{ij}| + |\hat{\mathbf{R}}_{ji}|}$ for non-zero values. Graph asymmetry is computed as the average relative difference of attention matrices. We compare SADE-GCN-sym and graph asymmetry in Table 4, and the results show that SADE-GCN outperforms SADE-GCN-sym on every dataset. This finding indicates that the asymmetric attention matrix is more effective.

4.2.3 the Robustness of Dual embedding Architecture

In this section, we conduct an experiment to verify the robustness of our dual embedding architecture. We add noise to the feature and topology respectively before training. For feature noise, we utilize the normal distribution and add it to the node feature using a coefficient range of [0.0, 0.3]. For topology noise, we randomly add or remove edges with a percentage range of [0, 0.3] of the original number of edges. We compare our SADE-GCN with three representative models: LINKX, GloGNN, and GCN. LINKX embeds feature and topology separately using MLPs, concatenate the embeddings, and feed them to the final MLPs. GloGNN combines the feature and topology embeddings using a weighted sum in the first layer. We demonstrate the results of Texas in Figure 2. We found that our model achieves higher accuracy than the others for different levels of noise, showing that independently and explicitly embedding features and topology during message passing can make the model more robust. The feature noise is more influential in this case than the topology noise since Texas relies more on features. For graphs dominated by topology, the impact of topology noise is higher. The results of other graphs are presented in the Appendix.

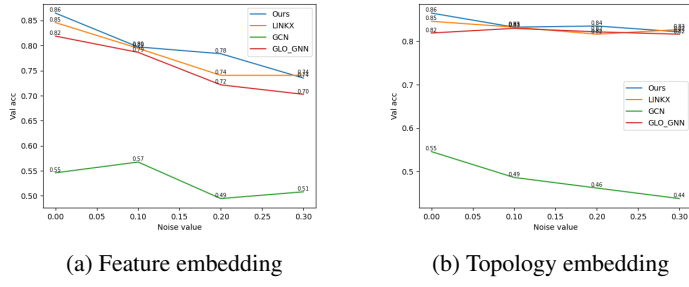


Figure 2: Embedding noise VS model accuracy (Texas)

5 Related Work

5.1 Graph Neural Network for Homophily and Heterophily

Here, we introduce several representative GNNs. Traditional GNNs are effective on homophilic graphs, but not on heterophilic graphs. GCN performs graph convolution with a degree-normalized adjacency matrix and learnable transformation weight [17]. GAT applies the attention mechanism to measure the importance of neighbor nodes during aggregation [29]. MixHop extends the aggregation to multi-hop neighbors for increased expressive ability [1]. Various GNNs have been designed to handle heterophilic graphs. Geom-GCN aggregates topology and latent space neighbors to maintain topology information and long-range dependencies for heterophilic graphs [22]. H_2 GNN is based on three design principles, including ego and neighbor separation, high-order neighbors, and multi-layer combination [43]. The weights contain positive and negative values, which help to learn both homophily and heterophily on the graph [4]. FAGCN first takes homophily and heterophily on the graphs as low and high frequency, respectively, and integrates different signals adaptively [2]. GGCN adjusts degree coefficients and gives a signed message to jointly solve over-smoothing and heterophily problems [34]. GloGNN and GloGNN++ use global feature similarity and topology similarity to conduct global message passing [18]. ACM-GCN has three frequency channels (high, low, identity) to extract graph signals, and ACM-GCN+ combines the embeddings from frequency channels with topology embeddings [21].

5.2 Graph Transformer

Transformer has achieved great success on the graph task. There are several kinds of Graph Transformers(GT). GraphBERT[40], apply self-attention mechanism without aggregation. It samples subgraphs within their local contexts for training efficiency. It can be used as a pre-trained model for downstream tasks. Graphomer[38] encodes the graph topology by novel, simple and effective methods. GPS[25] consists of positional and topology embedding, local message-passing, and global attention and keeps a balance between global and local information. GT has high parallelism and mitigates over-smoothing and over-squashing problems. In our method, we propose a novel self-attention mechanism inspired by GT to capture the heterophily and asymmetry of graphs.

6 Conclusion

In conclusion, we make three observations and corresponding analyses on heterophilic graphs. Firstly, we found that graph features and topology have varying degrees of importance and should be explicitly and independently embedded during message passing. Secondly, we discover that negative attention weights can be used to extract heterophily from both topology and feature embedding. Lastly, we identify the asymmetry present in heterophilic graphs. Based on these observations, we propose SADE-GCN, which explicitly encodes feature and topology through two independent paths and extracts heterophily and asymmetry through a novel self-attention mechanism. Our results show that SADE-GCN outperforms other models on heterophilic graphs and remains competitive on homophilic graphs. In future research, we plan to develop new sampling methods based on the heterophily and homophily of graphs to scale our model to larger graphs.

References

- [1] Sami Abu-El-Haija, Bryan Perozzi, Amol Kapoor, Nazanin Alipourfard, Kristina Lerman, Hrayr Harutyunyan, Greg Ver Steeg, and Aram Galstyan. Mixhop: Higher-order graph convolutional architectures via sparsified neighborhood mixing. In *international conference on machine learning*, pages 21–29. PMLR, 2019.
- [2] Deyu Bo, Xiao Wang, Chuan Shi, and Huawei Shen. Beyond low-frequency information in graph convolutional networks. In *Proceedings of the AAAI Conference on Artificial Intelligence*, volume 35, pages 3950–3957, 2021.
- [3] Ming Chen, Zhewei Wei, Zengfeng Huang, Bolin Ding, and Yaliang Li. Simple and deep graph convolutional networks. In *International conference on machine learning*, pages 1725–1735. PMLR, 2020.
- [4] Eli Chien, Jianhao Peng, Pan Li, and Olgica Milenkovic. Adaptive universal generalized pagerank graph neural network. *arXiv preprint arXiv:2006.07988*, 2020.
- [5] Alexey Dosovitskiy, Lucas Beyer, Alexander Kolesnikov, Dirk Weissenborn, Xiaohua Zhai, Thomas Unterthiner, Mostafa Dehghani, Matthias Minderer, Georg Heigold, Sylvain Gelly, et al. An image is worth 16x16 words: Transformers for image recognition at scale. *arXiv preprint arXiv:2010.11929*, 2020.
- [6] Yingtong Dou, Zhiwei Liu, Li Sun, Yutong Deng, Hao Peng, and Philip S Yu. Enhancing graph neural network-based fraud detectors against camouflaged fraudsters. In *Proceedings of the 29th ACM International Conference on Information & Knowledge Management*, pages 315–324. IEEE, 2020.
- [7] Vijay Prakash Dwivedi and Xavier Bresson. A generalization of transformer networks to graphs. *arXiv preprint arXiv:2012.09699*, 2020.
- [8] Zheng Fang, Lingjun Xu, Guojie Song, Qingqing Long, and Yingxue Zhang. Polarized graph neural networks. In *Proceedings of the ACM Web Conference 2022*, pages 1404–1413, 2022.
- [9] Will Hamilton, Zhitao Ying, and Jure Leskovec. Inductive representation learning on large graphs. *Advances in neural information processing systems*, 30, 2017.
- [10] Dongxiao He, Chundong Liang, Huixin Liu, Mingxiang Wen, Pengfei Jiao, and Zhiyong Feng. Block modeling-guided graph convolutional neural networks. In *Proceedings of the AAAI Conference on Artificial Intelligence*, volume 36, pages 4022–4029, 2022.
- [11] Kaiming He, Xinlei Chen, Saining Xie, Yanghao Li, Piotr Dollár, and Ross Girshick. Masked autoencoders are scalable vision learners. In *Proceedings of the IEEE/CVF Conference on Computer Vision and Pattern Recognition*, pages 16000–16009, 2022.
- [12] Kaiming He, Xiangyu Zhang, Shaoqing Ren, and Jian Sun. Deep residual learning for image recognition. In *Proceedings of the IEEE Conference on Computer Vision and Pattern Recognition (CVPR)*, June 2016.
- [13] Di Jin, Zhizhi Yu, Cuiying Huo, Rui Wang, Xiao Wang, Dongxiao He, and Jiawei Han. Universal graph convolutional networks. *Advances in Neural Information Processing Systems*, 34:10654–10664, 2021.
- [14] John Jumper, Richard Evans, Alexander Pritzel, Tim Green, Michael Figurnov, Olaf Ronneberger, Kathryn Tunyasuvunakool, Russ Bates, Augustin Žídek, Anna Potapenko, et al. Highly accurate protein structure prediction with alphafold. *Nature*, 596(7873):583–589, 2021.
- [15] Jinwoo Kim, Dat Nguyen, Seonwoo Min, Sungjun Cho, Moontae Lee, Honglak Lee, and Seunghoon Hong. Pure transformers are powerful graph learners. *Advances in Neural Information Processing Systems*, 35:14582–14595, 2022.
- [16] Diederik P Kingma and Jimmy Ba. Adam: A method for stochastic optimization. *arXiv preprint arXiv:1412.6980*, 2014.

- [17] Thomas N Kipf and Max Welling. Semi-supervised classification with graph convolutional networks. *arXiv preprint arXiv:1609.02907*, 2016.
- [18] Xiang Li, Renyu Zhu, Yao Cheng, Caihua Shan, Siqiang Luo, Dongsheng Li, and Weining Qian. Finding global homophily in graph neural networks when meeting heterophily. In *International Conference on Machine Learning*, pages 13242–13256. PMLR, 2022.
- [19] Valerii Likhoshevstov, Krzysztof Choromanski, and Adrian Weller. On the expressive power of self-attention matrices, 2021.
- [20] Derek Lim, Felix Hohne, Xiuyu Li, Sijia Linda Huang, Vaishnavi Gupta, Omkar Bhalerao, and Ser Nam Lim. Large scale learning on non-homophilous graphs: New benchmarks and strong simple methods. *Advances in Neural Information Processing Systems*, 34:20887–20902, 2021.
- [21] Sitao Luan, Chenqing Hua, Qincheng Lu, Jiaqi Zhu, Mingde Zhao, Shuyuan Zhang, Xiao-Wen Chang, and Doina Precup. Revisiting heterophily for graph neural networks. In *Advances in Neural Information Processing Systems*.
- [22] Hongbin Pei, Bingzhe Wei, Kevin Chen-Chuan Chang, Yu Lei, and Bo Yang. Geom-gcn: Geometric graph convolutional networks. In *International Conference on Learning Representations*.
- [23] Jorge Pérez, Pablo Barceló, and Javier Marinkovic. Attention is turing complete. *The Journal of Machine Learning Research*, 22(1):3463–3497, 2021.
- [24] Jorge Pérez, Javier Marinković, and Pablo Barceló. On the turing completeness of modern neural network architectures. *arXiv preprint arXiv:1901.03429*, 2019.
- [25] Ladislav Rampášek, Michael Galkin, Vijay Prakash Dwivedi, Anh Tuan Luu, Guy Wolf, and Dominique Beaini. Recipe for a general, powerful, scalable graph transformer. *Advances in Neural Information Processing Systems*, 35:14501–14515, 2022.
- [26] Prithviraj Sen, Galileo Namata, Mustafa Bilgic, Lise Getoor, Brian Galligher, and Tina Eliassi-Rad. Collective classification in network data. *AI magazine*, 29(3):93–93, 2008.
- [27] Andrew W Senior, Richard Evans, John Jumper, James Kirkpatrick, Laurent Sifre, Tim Green, Chongli Qin, Augustin Žídek, Alexander WR Nelson, Alex Bridgland, et al. Improved protein structure prediction using potentials from deep learning. *Nature*, 577(7792):706–710, 2020.
- [28] Ashish Vaswani, Noam Shazeer, Niki Parmar, Jakob Uszkoreit, Llion Jones, Aidan N Gomez, Łukasz Kaiser, and Illia Polosukhin. Attention is all you need. *Advances in neural information processing systems*, 30, 2017.
- [29] Petar Veličković, Guillem Cucurull, Arantxa Casanova, Adriana Romero, Pietro Liò, and Yoshua Bengio. Graph attention networks. In *International Conference on Learning Representations*.
- [30] Bingzhe Wu, Jintang Li, Chengbin Hou, Guoji Fu, Yatao Bian, Liang Chen, and Junzhou Huang. Recent advances in reliable deep graph learning: Adversarial attack, inherent noise, and distribution shift. *arXiv preprint arXiv:2202.07114*, 2022.
- [31] Felix Wu, Amauri Souza, Tianyi Zhang, Christopher Fifty, Tao Yu, and Kilian Weinberger. Simplifying graph convolutional networks. In *International conference on machine learning*, pages 6861–6871. PMLR, 2019.
- [32] Junjie Xu, Enyan Dai, Xiang Zhang, and Suhang Wang. Hp-gnn: Graph memory networks for heterophilous graphs. *arXiv preprint arXiv:2210.08195*, 2022.
- [33] Keyulu Xu, Chengtao Li, Yonglong Tian, Tomohiro Sonobe, Ken-ichi Kawarabayashi, and Stefanie Jegelka. Representation learning on graphs with jumping knowledge networks. In *International conference on machine learning*, pages 5453–5462. PMLR, 2018.
- [34] Yujun Yan, Milad Hashemi, Kevin Swersky, Yaoqing Yang, and Danai Koutra. Two sides of the same coin: Heterophily and oversmoothing in graph convolutional neural networks. In *2022 IEEE International Conference on Data Mining (ICDM)*, pages 1287–1292, 2022.

- [35] Han Yang, Kaili Ma, and James Cheng. Rethinking graph regularization for graph neural networks. In *Proceedings of the AAAI Conference on Artificial Intelligence*, volume 35, pages 4573–4581, 2021.
- [36] Liang Yang, Mengzhe Li, Liyang Liu, Chuan Wang, Xiaochun Cao, Yuanfang Guo, et al. Diverse message passing for attribute with heterophily. *Advances in Neural Information Processing Systems*, 34:4751–4763, 2021.
- [37] Liang Yang, Wenmiao Zhou, Weihang Peng, Bingxin Niu, Junhua Gu, Chuan Wang, Xiaochun Cao, and Dongxiao He. Graph neural networks beyond compromise between attribute and topology. In *Proceedings of the ACM Web Conference 2022*, pages 1127–1135, 2022.
- [38] Chengxuan Ying, Tianle Cai, Shengjie Luo, Shuxin Zheng, Guolin Ke, Di He, Yanming Shen, and Tie-Yan Liu. Do transformers really perform badly for graph representation? *Advances in Neural Information Processing Systems*, 34:28877–28888, 2021.
- [39] Seongjun Yun, Minbyul Jeong, Raehyun Kim, Jaewoo Kang, and Hyunwoo J Kim. Graph transformer networks. *Advances in neural information processing systems*, 32, 2019.
- [40] Jiawei Zhang, Haopeng Zhang, Congying Xia, and Li Sun. Graph-bert: Only attention is needed for learning graph representations. *arXiv preprint arXiv:2001.05140*, 2020.
- [41] Tong Zhao, Yozen Liu, Leonardo Neves, Oliver Woodford, Meng Jiang, and Neil Shah. Data augmentation for graph neural networks. In *Proceedings of the aaai conference on artificial intelligence*, volume 35, pages 11015–11023, 2021.
- [42] Elena Zheleva and Lise Getoor. To join or not to join: the illusion of privacy in social networks with mixed public and private user profiles. In *Proceedings of the 18th international conference on World wide web*, pages 531–540, 2009.
- [43] Jiong Zhu, Yujun Yan, Lingxiao Zhao, Mark Heimann, Leman Akoglu, and Danai Koutra. Beyond homophily in graph neural networks: Current limitations and effective designs. *Advances in Neural Information Processing Systems*, 33:7793–7804, 2020.

Appendix A Algorithm

A.1 Training Process of SADE-GCN

We give an algorithm to summary the training process of SADE-GCN in Algorithm 1.

Algorithm 1 SADE-GCN Training

```

1: Input  $\mathbf{A}$ ,  $\mathbf{X}$ ,  $\mathbf{Y}_{\mathcal{T}}$ , and a SADE-GCN model  $M$  with feature embedding path  $\mathbf{P}_f$  and topology
   embedding path  $\mathbf{P}_t$ 
2: for  $e = 1, 2, \dots, \text{epochs}$  do
3:   for  $l = 1, 2, \dots, L$  do
4:     if  $e \% U == 0$  then
5:       Update  $\tilde{\mathbf{A}}_f^{(l)}$  for  $\mathbf{P}_f$  and  $\tilde{\mathbf{A}}_t^{(l)}$  for  $\mathbf{P}_t$  in equation (4)(5)(6)(7).
6:     end if
7:     Do heterophilic graph convolution in  $\mathbf{P}_f$  and  $\mathbf{P}_t$  in equation (8)(9).
8:   end for
9:   Adaptively combine feature and topology embeddings in equation (10).
10:  Calculate cross entropy loss for training.
11: end for

```

Here is a time complexity analysis of SADE-GCN. The forward propagation of the network is from 2 to 11 lines of the above algorithm. We set the hidden dim as H . Updating $\tilde{\mathbf{A}}_t^{(l)}$ and $\tilde{\mathbf{A}}_f^{(l)}$ costs $\mathcal{O}(NH^2 + N^2H)$. Do heterophilic graph convolution costs $\mathcal{O}(N^2H + NH^2)$. Combining feature and topology costs $\mathcal{O}(NC^2)$. Since there are L layers, the total time complexity is $\mathcal{O}((NH^2 + N^2H + NC^2)L)$.

A.2 An Efficient Implementation for Graphs with Heterophily

In most cases, the amount of graph nodes N is much larger than the hidden dimension H and the number of classes C . In those cases, the time and space complexity is dominated by the calculation of attention matrix. The complexity of computing the attention matrix is quadratic in N . For some large datasets like arXiv-year, twitch-gamers .etc, the inner product of Q and K matrix tends to cause the OOM problem. In order to make it possible for GPU training and speed up calculations, we give an efficient algorithm for computing the attention matrix.

The implementation is as follows.

Algorithm 2 Efficient Self-attention for Graphs with Heterophily

```

1:  $Src(\tilde{\mathbf{A}})$  and  $Dst(\tilde{\mathbf{A}})$  represent the source node and destination node index of edges.
2: Arrange  $\mathbf{Q}^{(l)}$  by  $Src(\tilde{\mathbf{A}})$  to get  $\hat{\mathbf{Q}}^{(l)} \in \mathbb{R}^{E \times H^{(l)}}$ , i.e. The  $i$  row of  $\hat{\mathbf{Q}}^{(l)}[i]$  corresponds to
    $\mathbf{Q}^{(l)}[Src(\tilde{\mathbf{A}})[i]]$ , for  $i \in [1, E]$  .
3:  $\hat{\mathbf{K}}^{(l)} \in \mathbb{R}^{E \times H^{(l)}}$  can be obtained in In the same way above.
4: Do Hadamard product between  $\hat{\mathbf{Q}}^{(l)}$  and  $\hat{\mathbf{K}}^{(l)}$ , and sum by row to get  $\mathbf{R}^{(l)}$  stored in a sparse
   format.
5: Use the scaling function as equation (6) to get the attention matrix  $\hat{\mathbf{R}}^{(l)}$  with negative value.
6: Get the reweighted adjacency matrix  $\tilde{\mathbf{A}}^{(l)}$  as equation (7).

```

Algorithm 2 shows that the complexity for updating $\tilde{\mathbf{A}}_t^{(l)}$ and $\tilde{\mathbf{A}}_f^{(l)}$ is $\mathcal{O}(NH^2 + EH)$. The complexity for heterophilic graph convolution is $\mathcal{O}(EH + NH^2)$. The total time complexity for SADE-GCN is $\mathcal{O}((NH^2 + EH + NC^2)L)$. Due to the fact that E is much smaller than N^2 in most cases, the implementation can significantly reduce training time and memory usage.

To demonstrate the necessity of our algorithm, we also measured the memory usage when using it in Experiment 5. We conducted all experiments on an RTX 3090 GPU with 24GB of memory. Across all four large datasets with hidden dimension set to 256, our efficient algorithm reduced the

memory usage to below 10GB at most, making our model suitable for most existing GPUs. Without the algorithm, it would be impossible to implement the model on such large datasets.

Table 5: GPU Memory Comparison of Whether Use Efficient Self-attention

Efficient Self-attention	Penn94	arXiv-year	genius	twitch-gamers
✓	4.45GB	4.59GB	9.60GB	6.18GB
✗	OOM	OOM	OOM	OOM

Appendix B Dataset

Cora, **Citeseer** and **Pubmed** are three citation graphs that commonly used as network benchmark datasets. In these graphs, nodes represent papers, and edges indicate the citation relationships between the paper. They use bag-of-words representations as the feature vectors of nodes. Each Node is given a label to represent the research field. Note that these datasets are homophilic graphs.

Chameleon and **Squirrel** are two Wikipedia pages on a specific topic. The nodes represent the web pages, edges are mutual links between pages. Node feature represents some informative nouns on the page. Nodes are divided into five categories based on monthly visits.

Cornell, **Texas**, and **Wisconsin** datasets are collected by Carnegie Mellon University and comprise web pages as nodes and hyperlinks as edges to connect them. The node feature of these datasets is represented by the web page content in terms of their words. They are labeled into five categories, namely student, project, course, staff, and faculty.

Film is the subgraph selected from the film-director-actor-writer network. Nodes represent actor, and the edges denotes the co-occurrence relationship on the same Wikipedia page. Node features are produced by the actors keywords in the Wikipedia pages. The task is to classify the actors into five categories.

Penn94 dataset is a social network derived from Facebook, wherein the nodes represent students who use the platform and the edges indicate the following relationship between them. The nodes are further categorized based on the gender of the student. The node features comprise major, second major/minor, dorm/house, year, and high school. [18]

arXiv-year is a citation network extracted from ogbn-arXiv. Nodes in arXiv-year represent papers and edges represent the citation relationship between papers. The labels of nodes represent their posting year. The features represent paper title and abstract. Different from Cora, Citeseer and Pubmed, arXiv-year is with high heterophily.

genius is a social network from genius.com, featuring nodes representing users and edges indicating the following relationship between them. Each node is labeled with a "gone" label, indicating if they are unusual users. The node feature is composed of expertise scores, contributions, and the roles of the user.

twitch-gamers is a social graph from Twitch, which is a streaming platform. Similar to Penn94 and genius, it represents the users and following between them on the platform. The node feature represent the number of accesses, the time of creation and update, language, life time and whether the account is alive. The task is to distinguish whether the user has explicit content.

Appendix C Hyper-parameters

In our method, we utilize different types of attention function to combine the value and residual embedding in SAGC (combine-vr) and weight feature and topology embedding in the output layer (combine-ft). Both combine-vr and combine-ft offer three types of attention functions. The first type is the function used in equation (9) (type 1), while the second type is the adaptive attention method used in [21] to combine different channel outputs (type 2). Finally, the third type lacks any attention function (type 3). For most graphs, α_V and α_I in equation (8) and α_f and α_t in equation (10) are set to 1. However, for Pubmed and Film datasets, setting α_t as zero during training results in better performance on the validation set. This indicates that on these datasets, topology can interfere with the expression of feature embedding and is not useful. For Film and twitch-gamer datasets,

α_V is set to zero, indicating that the message-passing mechanism fails to perform on these graphs. Additionally, we can introduce non-linear layers and biases to $\mathbf{H}^{(l-1)}\mathbf{W}_I^{(l)}$ for better performance.

Next we introduce hyper-parameters we choose for training. For training process, the maximum epochs is in $\{60, 220, 240, 300, 390, 500, 1800, 2100\}$. The searching range of learning rate is $\{1e-3, 2e-3, 5e-3, 1.5e-2, 2e-2, 1e-2, 5e-2, 6e-2\}$, the weight decay ranges in $\{0.0, 1e-5, 2e-5, 5e-5, 1e-4, 2e-4, 5e-4, 1e-3, 2e-3, 5e-3, 1e-1\}$. Dropout is in $\{0.0, 0.1, 0.2, 0.3, 0.6, 0.7, 0.8, 0.9\}$. U in $\{1, 5, 10, 20, 50, 100, 240, 250\}$ is the epoch interval to update the attention matrix. For each training, we choose the model parameters with highest validation accuracy/ lowest validation loss.

The hyper-parameters of SADE-GCN on each graph are shown as Table 6 and Table 7.

Table 6: The hyper-parameters of the nine small graphs.

	Cora	Citeseer	Pubmed	Squirrel	Chameleon	Texas	Wisconsin	Cornell	Film
combine-vr	2	2	2	2	1	2	2	2	2
combine-ft	2	1	3	3	1	2	3	2	1
α_V	1	1	1	1	1	1	1	1	0
α_I	1	1	1	1	1	1	1	1	1
α_f	1	1	1	1	1	1	1	1	1
α_t	1	1	0	1	1	1	1	1	0
non-linear	0	0	0	0	0	0	0	0	1
bias	0	1	0	1	0	1	1	0	1
epochs	220	60	240	1800	300	500	2100	390	500
dropout	0.6	0.7	0.3	0.8	0.8	0.1	0.1	0.1	0.0
learning rate	$2e-3$	$1e-2$	$6e-2$	$2e-3$	$5e-2$	$1.5e-2$	$1.5e-2$	$1e-2$	$1e-2$
weight decay	$2e-4$	$5e-5$	$1e-5$	$1e-4$	$1e-4$	$5e-4$	$2e-4$	$5e-4$	$2e-3$
U	5	20	240	50	10	10	5	10	500

Table 7: The hyper-parameters of the four large graphs.

	Penn94	arXiv-year	genius	twitch-gamers
combine-vr	2	2	2	2
combine-ft	2	2	2	2
α_V	1	1	1	0
α_I	1	1	1	1
α_f	1	1	1	1
α_t	1	1	1	1
non-linear	0	0	1	0
bias	0	0	1	0
epochs	500	500	500	500
dropout	0.5	0.7	0.0	0.9
learning rate	$1e-3$	$5e-3$	$5e-3$	$1e-3$
weight decay	$1e-1$	$1e-3$	0.0	$1e-2$
U	10	10	10	100

Appendix D Experimental Results

D.1 Heterophily vs K-Hop Embedding Distance

In this study, we present an experiment to demonstrate how our SADE-GCN model can extract graph heterophily from both feature and topology, highlighting the necessity of using a Self-attention mechanism to merge the embeddings.

By defining strict K-hop neighbors as nodes whose graph distances are equal to K, we can calculate the K-hop homophily, which is the ratio of K-hop neighbors sharing the same label. Additionally, we can measure the K-hop feature and topology embedding distance by computing the cosine distance¹

¹<https://docs.scipy.org/doc/scipy/reference/generated/scipy.spatial.distance.cosine.html>

between the feature and topology embeddings of a node and its K-hop neighbors, where the cosine distance serves as an effective similarity measure ranging from 0 to 2.

To showcase the effectiveness of our approach, we present results for each graph that indicate the K-hop homophily, K-hop feature embedding distance, and K-hop topology embedding distance. We represent feature and topology embeddings of nodes using $\mathbf{H}_f^{(L)}$ and $\mathbf{H}_t^{(L)}$, respectively. Note that for some small datasets like Wisconsin or Cornell, the high-order neighbor distance falls to 0. This is because no neighbor in this order for each of the nodes in the graph.

From the figures, we can make the following observations: Generally, all the figures follow the rule that when the homophily is high, the feature/structure distance is small, and vice versa. For homophily graphs like Cora and Citeseer, The farther away the neighbors are, the greater the embedding distance. For other heterophily graphs, the distance changes with homophily. This is reasonable because high homophily indicates neighbor nodes tend to be in the same class, so their feature/topology similarity should be higher, and the distance is smaller. These results also show that our model can mine into intrinsic heterophily of datasets.

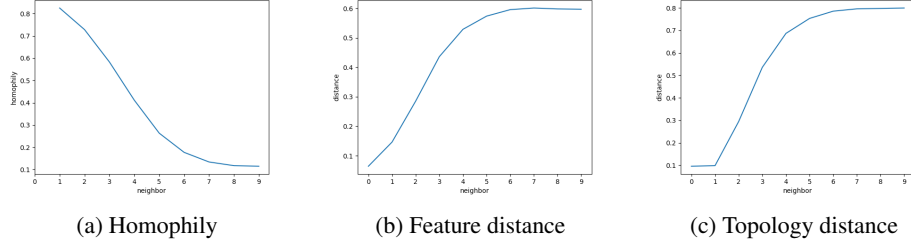


Figure 3: Homophily and Feature/Topology embedding distance (Cora)

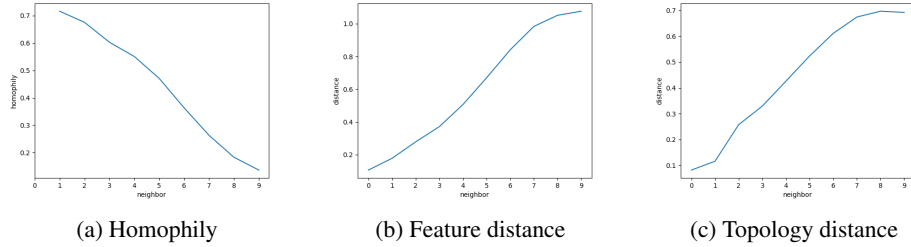


Figure 4: Homophily and Feature/Topology embedding distance (Citeseer)

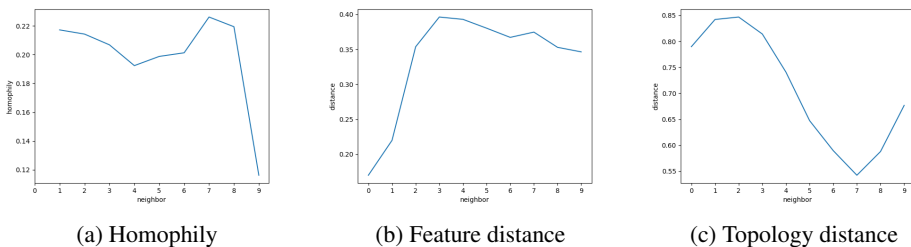


Figure 5: Homophily and Feature/Topology embedding distance (Squirrel)

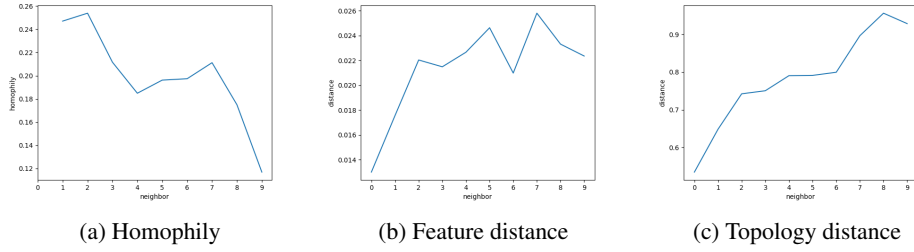


Figure 6: Homophily and Feature/Topology embedding distance (Chameleon)

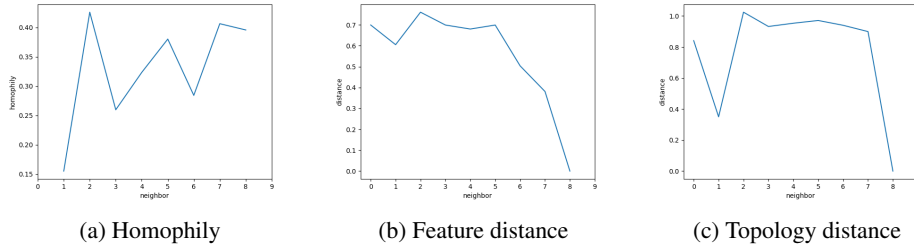


Figure 7: Homophily and Feature/Topology embedding distance (Wisconsin)

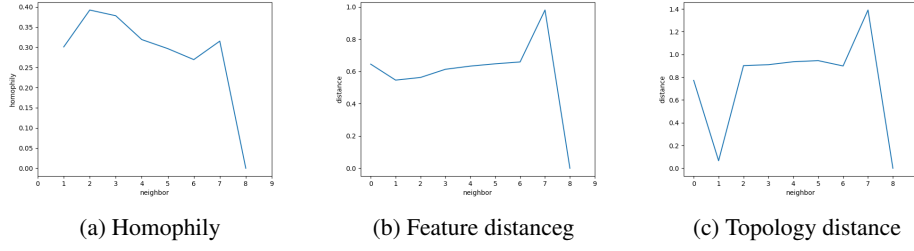


Figure 8: Homophily and Feature/Topology embedding distance (Cornell)

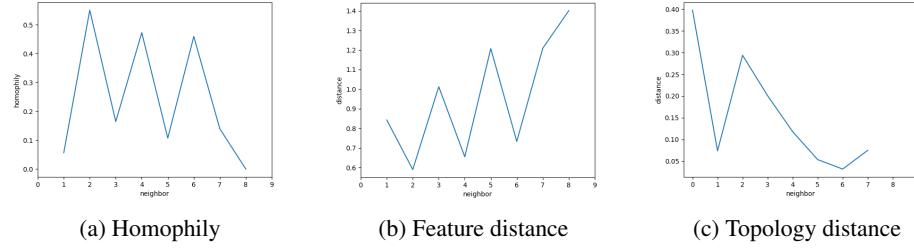
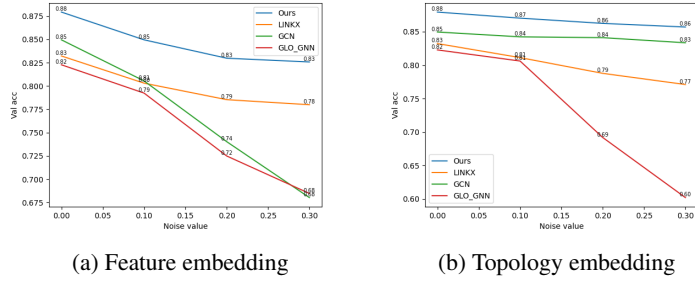


Figure 9: Homophily and Feature/Topology embedding distance (Texas)

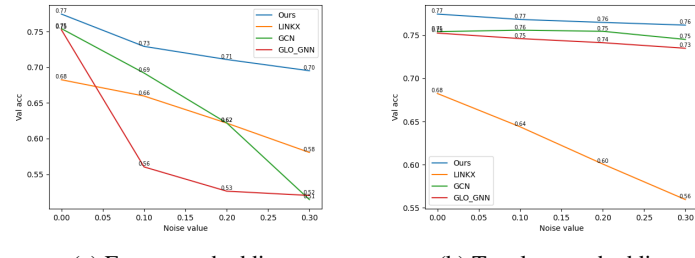
D.2 the Robustness of Dual Embedding Architecture

In Section 4.2.3, we demonstrate an experiment to verify the robustness on Texas. Here is the results of other graphs for the experiment. The Figures 1011121314 thoroughly verify the arguments we put forward, i.e. independently and explicitly embedding feature and topology during message passing can make the model more robust.



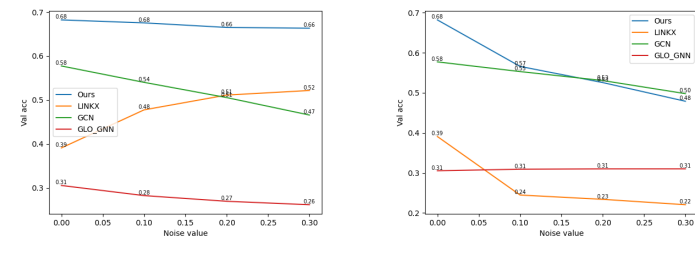
(a) Feature embedding (b) Topology embedding

Figure 10: Embedding noise VS model accuracy (Cora)



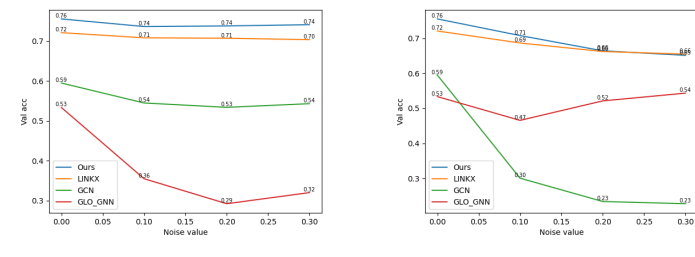
(a) Feature embedding (b) Topology embedding

Figure 11: Embedding noise VS model accuracy (Citeseer)



(a) Feature embedding (b) Topology embedding

Figure 12: Embedding noise VS model accuracy (Squirrel)



(a) Feature embedding (b) Topology embedding

Figure 13: Embedding noise VS model accuracy (Chameleons)

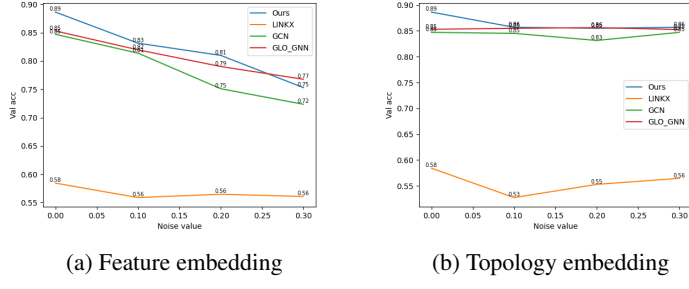


Figure 14: Embedding noise VS model accuracy (Wisconsin)

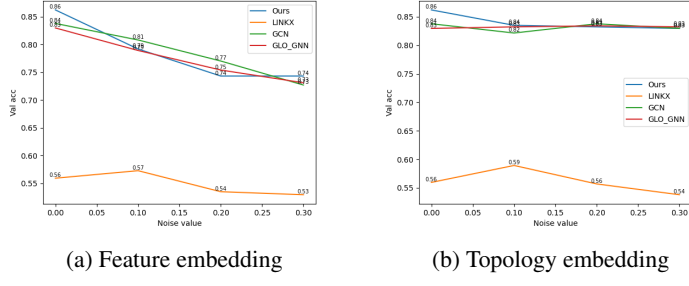


Figure 15: Embedding noise VS model accuracy (Cornell)

Appendix E Code

Our code will be available soon. For data preprocessing, we refer to GloGNN[18] and ACM-GNN[21]. Their code can be found in ² and ³.

²<https://github.com/RecklessRonan/GloGNN>

³<https://github.com/SitaoLuan/ACM-GNN>